Published in final edited form as:
Int J Radiat Oncol Biol Phys. 2008 December 1; 72(5): 1385–1395. doi:10.1016/j.ijrobp.2008.03.007.

EFFECTS OF INTERFRACTIONAL MOTION AND ANATOMIC CHANGES ON PROTON THERAPY DOSE DISTRIBUTION IN LUNG CANCER

Zhouguang Hui, M.D.[*], **Xiaodong Zhang, Ph.D.**[*], **George Starkschall, Ph.D.**[*], **Yupeng Li, M.S.**[*], **Radhe Mohan, Ph.D.**[*], **Ritsuko Komaki, M.D.**[†], **James D. Cox, M.D.**[†], and **Joe Y. Chang, M.D., Ph.D.**[†]

[*]Department of Radiation Phyiscs, The University of Texas M. D. Anderson Cancer Center, Houston, TX

[†]Department of Radiation Oncology, The University of Texas M. D. Anderson Cancer Center, Houston, TX

Abstract

Purpose—Proton doses are sensitive to intra- and interfractional anatomic changes. We analyzed the effects of interfractional anatomic changes in doses to lung tumors treated with proton therapy.

Methods and Materials—Weekly four-dimensional computed tomography (4D-CT) scans were acquired for 8 patients with mobile Stage III non–small cell lung cancer who were actually treated with intensity-modulated photon radiotherapy. A conformal proton therapy passive scattering plan was designed for each patient. Dose distributions were recalculated at end-inspiration and end-expiration breathing phases on each weekly 4D-CT data set using the same plans with alignment based on bone registration.

Results—Clinical target volume (CTV) coverage was compromised (from 99% to 90.9%) in 1 patient because of anatomic changes and motion pattern variation. For the rest of the patients, the mean CTV coverage on the repeated weekly 4D-CT data sets was 98.4%, compared with 99% for the original plans. For all 8 patients, however, a mean 4% increase in the volume of the contralateral lung receiving a dose of at least 5 Gy (V5) and a mean 4.4-Gy increase in the spinal cord maximum dose was observed in the repeated 4D-CT data sets. A strong correlation between the CTV density change resulting from tumor shrinkage or anatomic variations and mean contralateral lung dose was observed.

Conclusions—Adaptive re-planning during proton therapy may be indicated in selected patients with non–small cell lung cancer. For most patients, however, CTV coverage is adequate if tumor motion is taken into consideration in the original simulation and planning processes.

Keywords

Lung cancer; Proton therapy; 4D CT; Intensity-modulated radiation therapy; Adaptive radiotherapy

Reprint requests to: Joe Y. Chang, MD, PhD, Department of Radiation Oncology, Unit 97, The University of Texas M. D. Anderson Cancer Center, 1515 Holcombe Boulevard, Houston, TX 77030. Tel: (713) 563-2337; Fax: (713) 563-2331; jychang@mdanderson.org.

Presented in abstract form during the Particle Therapy Co-Operative Group (PTCOG), Zibo, China, May 18–23, 2007, and American Society for Therapeutic Radiology and Oncology Annual Meeting, Los Angeles, CA, October 28–November 1, 2007.

Conflict of interest: none.

INTRODUCTION

Lung cancer is the leading cause of cancer-related mortality and conventional photon radiotherapy is associated with less than 50% local control. Dose escalation has been shown to improve local control and possibly survival, but it is associated with increased toxicity, particularly when concurrent chemotherapy is given (1).

Clinical proton beams, unlike X-ray beams, can be delivered in such a way that the radiation dose that enters the body is low, followed by a region of uniformly high dose (the spread-out Bragg peak [SOBP]) at the tumor/target, and then a steep fall-off to zero dose (2). These characteristics make possible a substantial reduction in the dose to normal tissues while maximizing the dose to the tumor and give proton therapy an inherent advantage over conformal photon therapy, particularly for lung cancer (3–8). Our recent virtual clinical trials study showed that proton therapy may potentially allow for dose escalation/acceleration without increasing side effects compared with three-dimensional (3-D) conformal photon therapy and intensity-modulated radiation therapy (IMRT) in early-stage and advanced-stage non–small cell lung cancer (NSCLC) (4). However, breathing causes lung and thoracic normal tissues and cancers to move during treatment, with 40% of the lung tumor moving more than 5 mm (10% moves >10 mm) (9), and proton doses are very sensitive to motion and anatomic changes. With the use of four-dimensional computed tomography (4D-CT), volumetric image data can be acquired at many different respiratory phases, and the time-related CT imaging allows organ motion to be characterized for treatment planning (10).

We and others have recently published studies analyzing proton therapy planning strategies for mobile lung cancer using 4D-CT simulation and planning (11, 12). We concluded that intrafractional tumor and normal tissue motion needed to be taken into consideration for each patient, particularly in customized proton compensator design. However the use of 4D-CT scans taken at the beginning of the proton therapy course does not eliminate all mobility-induced errors because tumor and normal anatomy can change significantly owing to daily positioning uncertainties and anatomic changes during the course of treatment as a result of the nonrigidity of the body, tumor shrinkage, and weight loss (13–15). Also, an individual lung cancer patient's breathing patterns can be complex and can exhibit considerable variation (16, 17). In fact, breathing patterns have been shown to vary during a conventional course of radiotherapy (17). If tumor motion increases between fractions, even a shrinking tumor volume can cause an enlarged target volume, since the target volume in our 4DCT technique is calculated using all possible tumor positions during a respiratory cycle.

Because proton therapy is more susceptible to tissue density uncertainties, including motion effect, than photon therapy (2–8), we wanted to know whether the use of highly conformal, high-dose proton therapy plans designed on the basis of a single 4D-CT data set acquired for planning purposes during the simulation would lead to unforeseen complications or marginal misses of target volumes owing to interfractional geometric uncertainties.

To our knowledge, this article is the first investigation of the dosimetric impact of interfractional movement of anatomy on proton therapy planning with weekly 4D-CT in patients with locally advanced NSCLC.

METHODS AND MATERIALS

Patient characteristics and study design

Eight patients with inoperable Stage IIIA/B mobile NSCLC were studied. The patients were chosen from the first 8 patients who were enrolled in our institutional review board–approved tumor motion protocol and underwent intensity-modulated photon radiotherapy in our thoracic service during 2004 to 2005. Original free-breathing CT and 4D-CT were performed for all patients to allow consideration of tumor motion in planning. The 4D-CT was repeated weekly to assess the intra- and interfractional movement of the target volumes as well as the normal structures during 7 weeks of treatment. The dosimetric consequences of movement over time were studied by projecting the dose distributions of the original plan onto the repeated 4D-CT scans.

4D-CT and target delineation

The 4D-CT scanning approach used at our center has been reported in detail (11, 18, 19). For the original plan, a fast free-breathing CT scan and a 4D-CT scan were acquired on a multislice helical CT scanner (Discovery ST, General Electric Healthcare, Wakesha WI). The average CT and maximum intensity projection (MIP) CT values were calculated using the mean and maximum CT numbers, respectively, of the 10 CT datasets (from 10 phases of breathing cycle) at each pixel location. The MIP CT scan represents the highest density in space in the path of all moving tissues among the 10 phases of the breathing cycle. The internal gross tumor volume (IGTV), defined as the envelope of the gross tumor volume (GTV) over the 10 phases of the 4D-CT data set, was delineated using the MIP technique and modified by visual verification of the target volume throughout the 10 breathing phases; the 10 phases were chosen on the basis of practical signal-to-noise ratio, reconstruction time, and radiation dose exposure (11). The clinical target volume (CTV) was defined as the IGTV plus an 8-mm margin for microscopic disease (20).

Patient alignment using skin markers and bone registration was used for the weekly 4D-CT and analyzed separately. The weekly 4D-CT–based CTV was first automatically created from the original planning CT image on the basis of bone registration and then modified on the basis of the weekly 4D-CT MIP images and verified through visual verification of the target volume throughout 10 breathing phases.

Treatment planning with initial CT images

A commercial treatment planning system (Eclipse; Varian Medical Systems, Inc., Palo Alto, CA) was used for proton therapy plans. The proton therapy plans were designed using a procedure recently developed at our institution (4, 11). The initial plan was created using the free-breathing CT scans, and it accounted for tumor motion by using the two extreme phases of the breathing cycle (the end of expiration and the end of inspiration).

The CTV (IGTV plus an 8-mm margin) was used for target volume design and PTV was used for target coverage evaluation. Dose was prescribed to the CTV to achieve at least 99% coverage. The prescribed dose was 63 Gy in 1.8 Gy/fraction. The lung V20, heart V40, esophagus V55, mean total lung dose, and maximum dose to the spinal cord were required to be less than 35%, 50%, 50%, 20 Gy, and 50 Gy, respectively. Typically, we started with posterior, lateral beams plus an oblique beam that avoids lung parenchyma in its exit dose. For each beam, we first designed an aperture block to project outside of the target by a distance determined from the user input parameter aperture margin (AM), as defined as a 50% to 90% proton penumbra. Then we calculated the water equivalent depths of the target distal edges with user-defined distal margin (DM) and proximal edges with user-defined proximal margin (PM) using Strategy 2 reported by Moyers *et al.* (21). Both DM and PM

were added to take into consideration the uncertainty in the proton plan. These depths determined the energy required to penetrate the most distal target edge with DM and the width of the SOBP. The SOBP was designed to cover the water equivalent depth between the most distal target edge with DM and the proximal target edge with PM. A compensator was then designed to shape the distal target edge as determined by IGTV MIP density plus DM. In proton treatment planning, uncertainty in alignment of the compensator to the patient and motion of the patient during the treatment can create “cold spots” in the target. To guarantee target coverage, the compensator was smeared out by specifying the smearing margin using Strategy 2 reported by Moyers *et al.*, referred to as bolus expansion by those authors (21). Because the compensator was designed by simple ray tracing through the target, and the compensator region not traced by the ray was set to the maximum thickness, protons scraped along the walls of the ray-tracing compensator where the compensator was not shielded by the block. To avoid this effect, a border-smoothing margin was introduced by Eclipse to set the compensator thickness *t* not shielded by the block to the average thickness of the compensator traced by ray and located within the circle centered at t with radius defined by the border-smoothing margin. In our proton treatment planning, 1 cm was usually used for the border-smoothing margin.

Two procedures were used to consider the respiration motion effects. First, the motion effect was explicitly taken into account by using 4D-CT to delineate the IGTV, as described above. Second, the initial design plan was verified using the end of inspiration and expiration phases of the 4D-CT data set. If the target coverage and endpoints of the critical region of interest calculated from the two extreme phases of the breathing cycle were substantially different from those calculated in the original planning CT, the smearing parameters were re-adjusted accordingly. In this study, the difference was considered substantial if it resulted in a more than 0.5% decrease in CTV coverage or if there was more than a 2% variation in the dose volume histograms of critical normal tissues.

Treatment planning with weekly 4D-CT images

For practical reasons, we elected to acquire weekly 4D-CT scans for each patient showing the two extreme phases of the breathing cycle, the end of expiration (expiration phase) and the end of inspiration (inspiration phase), to represent the uncertainties caused by respiration motion during the whole respiratory cycle. Skin marker registration was performed before each weekly CT scan. For each patient, we selected 14 sets of CT images (one expiration phase and one inspiration phase) acquired during the 7-week treatment, and two sets of initial 4D-CT images (expiration and inspiration phase) acquired for treatment planning at the time of simulation.

The dose distributions were recalculated on the basis of the inspiration and expiration phase weekly CT images using the same beam portals (*i.e.*, the same beam range, SOBP width, aperture, range compensators, and normalization) with either skin marker or bone registration. To evaluate the target coverage during 7 weeks of radiotherapy, we calculated the average percentage of the CTV receiving the prescribed dose or higher for each of the seven expiration/inspiration phase CTs. For normal tissue dose, we calculated dose volume histograms based on the clinical significance of each critical organ. Dose distributions were evaluated by analyzing isodose displays, dose–volume histograms (DVHs), and target coverage. A total of 136 proton treatment plans (16 plans for each of the 8 patients) using bone registration plus 112 plans (14 plans for each of the 8 patients) using skin marker registration were conducted and analyzed. In selected cases, intensity-modulated radiation (photon) therapy (IMRT) planning was conducted as a comparison.

RESULTS

As shown in Table 1, our average original proton treatment plans adequately covered the CTV with minimal variation in normal tissue doses, as confirmed by the expiration and inspiration phase data sets. The verification plans using 4-D-generated images in the expiration/inspiration phase using a simulated CT data set showed that average and individual CTV coverage remained at about 99%, indicating that our original plan was sufficient to take intrafractional tumor motion into consideration.

When the original plans were applied to weekly 4D-CT images over 7 weeks in all 8 patients, CTV coverage was compromised in selected cases. Particularly, alignment using skin markers only during the 7 weeks of proton therapy resulted in substantial CTV target misses, although variation in the normal tissue DVHs remained within 2.4% (Table 2). The average CTV coverage dropped from 99% to 95%, with some cases having as little as 75.5% coverage. However, the average and individual CTV coverage was higher (97.9%) when alignment using bony structures, rather than skin markers only, was used, indicating the crucial role of a daily on-board X-ray image (Table 2). The CTV prescription coverage in the repeated 4D-CT plans using bony structure alignment was, however, as low as 90.9% for 1 patient because of anatomic changes and motion variation during the 7 weeks of treatment (see Discussion).

Using bony registration, the total lung V5, V20, and V30 values and the mean dose increased by 2.2%, 1.4%, 1.3%, and 0.7 Gy, respectively, compared with original planning at simulation, over 7 weeks of treatment. The heart V40 increased by 1.5%, and the esophagus V55 increased by 0.8%. Among the normal tissues, the spinal cord maximum dose exhibited the largest variation, increasing by 4.4 Gy. The average DVH variation between the original plan and the weekly 4D-CT plans was within 2.5%. When the expiration phase and inspiration phase dose distributions in the repeated plans were compared, the V5, V20, V30, and mean dose in the lung were consistently higher in the former, which was as expected because the lung volume is larger in the inspiration phase than in the expiration phase. This difference in dose distribution between the two breath phases was not seen in the CTV or in other normal tissues. In addition, compared with ipsilateral lung, the increase of the V5, V20, V30, and mean dose over 7 weeks was higher in the contralateral lung.

A representative case showing typical isodose distributions in the transverse and sagittal planes of the planning CT data set and 7 weekly CT data sets in the expiration and inspiration phases is shown in Fig. 1A. The prescription dose lines (yellow) did not show large variation among the seven weekly CT data sets in either the expiration or inspiration phase. The 10-Gy line only appeared at the anterior region of the contralateral lung in the planning CT data sets, but spread to other contralateral lung regions in the weekly CT data sets. The 45 Gy and 20 Gy lines also showed some variation at the anterior region of the contralateral lung but exhibited little variation in other regions. In the sagittal planes of the inspiration phase CT data set, the diaphragm position varied widely, which indicates the irregularity of the patients' breathing during the course of the treatment.

Figure 1B shows the DVHs of CTV and normal tissues for the representative case and their variation (DVH variation band shown as the shaded region) over 7 weeks of repeated 4D-CT plans. The DVH variation band for the CTV was very narrow, just outside the original DVH line. The DVH variation for the contralateral lung was above the original DVH lines, whereas the DVH variation bands for the total lung and ipsilateral lung were symmetrically distributed around the original DVH lines. The DVH variation bands for the spinal cord, heart, and esophagus were also wide and consistently above the original DVH lines, which

means that the irradiated volume of these organs was often larger in the repeated 4D-CT plans than in the original plan. These data show minimal variation in CTV coverage but a systematic increase in dose to the contralateral lung, heart, spinal cord, and esophagus in a typical case over 7 weeks of radiotherapy.

Because proton dose is very sensitive to changes in density, and because tumor density may change during 7 weeks of treatment, we analyzed the correlation between the CTV density change resulting from tumor shrinkage or anatomic variation and the normal tissue DVHs histograms. In Fig. 1C, we plotted the scaled average density of CTV and the scaled mean dose to the contralateral lung for the representative patient during the 7 weeks of radiotherapy. For all endpoints, the scaled endpoint for each week was calculated by dividing the value of the weekly endpoint by the value of the endpoint for the first week. The scaled endpoint is used to bring different endpoints to the same scale in one graph to show the correlation between two or more endpoints. Interestingly, the CTV density fluctuated over 7 weeks. Over the first 3 weeks of treatment, radiation may have caused the tumor to shrink, resulting in a decrease in the CTV density. However the CTV density appeared to increase from week 3 to week 4 before continuously decreasing again, with small fluctuations. The increase in CTV density may have been caused by radiation-induced inflammation, and the fluctuation in CTV density over the 7 weeks of radiotherapy may have been caused by the combined effects of tumor shrinkage and radiation-induced inflammation. There was a close inverse correlation between average CTV density and contralateral lung mean dose over 7 weeks of treatment with proton therapy planning. However there was no such trend or correlation in the same patient when IMRT (photon) therapy planning was conducted, indicating that protons are much more sensitive to density changes than photons (Fig. 1C). When data from all 8 patients were analyzed, a similar trend for inverse correlation between CTV density and contralateral lung mean dose was observed (Figs. 2a, 2b). The correlation between CTV density and other critical structures, such as the spinal cord, heart, esophagus, and ipsilateral lung, for all 8 patients is also shown in Figs. 2c to 2f. The spinal cord maximum dose continued to increase, whereas the heart V40, esophagus V55, and ipsilateral lung mean dose exhibited relatively smaller fluctuations.

Figure 3 shows a case involving compromised CTV coverage resulting from interfractional tumor motion and anatomic changes. Although the patient was aligned on the basis of bony structures, a substantial alignment error was observed for the GTV and CTV over soft tissue in Week 7 (Fig. 3a). When proton therapy planning was conducted, compromised CTV and IGTV coverage was observed, with the prescription isodose line (63 Gy, yellow line) broken over GTV and CTV and substantial increased contralateral lung dose. As shown in Fig. 3c, coverage of the CTV was reduced from 99% to 90.9%, and the contralateral lung and esophagus dose increased between the planned DVH and the DVH calculated at Week 7. However, when IMRT planning was conducted, there was no reduction in IGTV and CTV coverage, and the contralateral lung dose was not increased (Fig. 3b).

DISCUSSION

It is known that proton dose is sensitive to anatomic changes and motion effects. To take these uncertainties into consideration, generous internal margins and smearing margins have been recommended for proton therapy planning (21, 22). However the most substantial cause of missing the treatment target is daily set-up uncertainty. As shown in our current study (Table 2), up to 25% of the CTV could be missed during 7 weeks of radiation therapy if set-up relies on skin markers only, compared with an up to 9% error using daily bone registration. These data show that it is crucial to acquire daily X-ray images to align the patient before each proton therapy treatment. Currently this is the common practice in proton therapy facilities.

We observed that target CTV coverage exhibited minimal variation (~99% coverage) in 7 of 8 patients during the course of the treatment if tumor motion was taken into consideration during the original proton therapy planning. This finding indicates that imaging during the original 4D-CT simulation can predict the pattern of tumor motion during the course of radiation therapy. However, in 1 case (Fig. 3), even though the patient was aligned using bone registration for the weekly treatment simulations, the CTV coverage was substantially compromised (from 99% to 90.9%). This reduction in CTV coverage was caused by the large variation between the original simulation 4D-CT image and the weekly 4D-CT image, indicating that bone registration is not adequate for some patients and that repeated 4D-CT imaging is indicated for proton therapy re-planning. Interestingly, when we conducted IMRT planning for the same patient, the motion/anatomic change during the 7 weeks of radiotherapy did not substantially compromise the CTV coverage, indicating that proton therapy is more sensitive than IMRT to motion and density changes.

Another concern during radiation therapy, in addition to missing the CTV, is normal tissue toxicity. For the current study, values for the total lung and ipsilateral lung V5, V20, and V30, heart V40, and esophagus V55 in repeated 4D-CT plans were within 2.5% of those for the original plans. However the contralateral lung V5, V20, and V30, values and spinal cord maximum dose exhibited larger variations. Recent data showed that contralateral lung dose, particularly V5, was correlated with severe lung toxicity (23). Therefore, it is clinically important to reduce the contralateral lung dose including V5. One major reason for those large variations is the unique uncertainties of proton dose distribution caused by tumor shrinkage. As shown in Fig. 1C, there was an inverse correlation between CTV density and contralateral lung mean dose in proton plans over the 7 weeks of radiation ther apy. However, when we designed an IMRT plan based on the simulation CT and recalculated the dose distribution for the repeated weekly 4D-CT scans, the variation in the CTV density did not cause a corresponding variation in the contralateral lung mean dose in the same patient, indicating that the contralateral lung mean dose is less sensitive to CTV density change in IMRT planning than in proton therapy planning.

Even in proton treatment, normal tissue toxicity could be a major concern if the target is close to critical structures and dose-escalated proton therapy is conducted. At the University of Texas M. D. Anderson Cancer Center, we are conducting a phase I/II clinical study of proton therapy to a total dose of 87.5 Gy in 35 fractions for Stage IB (T2N0M0), centrally located stage IA (T1N0M0), and selected Stage II (T3 [chest wall involvement] N0M0) NSCLC and 74 Gy in 37 fractions with concurrent chemotherapy for inoperable Stage III NSCLC (8). Particularly at a dose of 87.5 Gy, toxicity could be a concern if critical structures such as the spinal cord, esophagus, or brachial plexus are close by. Figure 4 shows a case of Stage I NSCLC from our clinical study involving a patient treated with dose escalated/accelerated proton therapy to 87.5 Gy. At 5 weeks, a repeated 4D-CT simulation shows dramatic shrinkage of the primary tumor that resulted in an unacceptable radiation dose to the brachial plexus. Adaptive re-planning keeps the CTV coverage adequate and the brachial plexus within the tolerated dose. In our clinical practice, it is standard practice to repeated 4DCT simulation after 3 weeks of proton therapy. The decision is then made as to whether adaptive re-planning or another simulation is needed.. For the hypo-fractionated (10–20 fractions) proton therapy in Stage I NSCLC as reported by others (24–26), tumor shrinkage during the therapy is less dramatic compared with our studies because the hypofractionated treatment was finished within 4 weeks instead of 7 weeks. However set-up accuracy becomes more crucial because of limited fractions.

The issue of whether we should treat a smaller volume if primary tumor shrinkage occurs during radiation therapy remains controversial (27). Some radiation oncologists are concerned about the potential for residual microscopic disease even if the gross tumor

responds. One of our recent studies (15) showed that tumor volume reduction ranged from 20% to 71% (end-inspiration) and from 15% to 70% (end-expiration) during 7 weeks of radiotherapy. Increased tumor mobility was observed in the superior–inferior and anterior–posterior directions. However, no trends in tumor motion were observed. A marginally significant ($p = 0.049$) increase in total GTV positional variation was observed with increasing treatment weeks. Bosmans *et al.* (28) did not observe a significant decrease in tumor volume during the first 2 weeks of radiotherapy using an accelerated fractionation schedule (1.8 Gy twice a day). They even observed that tumor volume increased for some patients. Kupelian *et al.* (29) observed that tumor volume decreased at a relatively constant rate for 10 patients with NSCLC treated with helical tomotherapy with a conventional fractionation schedule. Our recent preliminary data showed substantial tumor shrinkage during 7 weeks of proton therapy and adapted planning was indicated (30).

In the current study, although CTV is typically modified on the basis of anatomic and motion changes of the GTV during 7 weeks of radiation therapy, the repeated 4D-CT–based CTV volumes were not intended to be reduced even if the GTV on repeated 4D-CTs shrank. Interestingly, for some cases, we observed that CTV density increased after 2 weeks of treatment, as shown in Fig. 2. Most likely, this increase in CTV density was caused by inflammation induced by radiation therapy. It remains debatable whether we should enlarge the CTV volume on the basis of the repeated 4D-CT scans. The optimal cut-off for proton re-planning if anatomic/motion changes only slightly during the 7 weeks of radiotherapy is also unknown. In our current clinical practice, we require adaptive re-planning if normal tissue toxicity is a concern clinically or if the CTV coverage is compromised by more than 2%. Currently we are conducting weekly 4D-CT scans of lung cancer patients undergoing proton therapy, and more information will be available soon. A study will be performed to compare the differences in tumor volume and the variations in density patterns between photon and proton therapy. Intensity-modulated proton therapy may spare more normal tissues than our current passive scattering approach (31). However intra- and interfractional tumor motion and anatomic changes have a more significant impact on treatment design than does the treatment approach. There fore, a 4D-CT–based intensity-modulated proton therapy study in mobile lung cancer is ongoing at our institution.

CONCLUSION

In summary, most target misses and/or increased normal tissue exposure are caused by daily set-up uncertainty, and daily on-board X-rays to align patients using bony structures is required in proton therapy. In most cases when patients are aligned using bony anatomy, there is no substantial compromise of tumor coverage and normal tissue sparing when the treatment plans are recalculated on repeated weekly 4D-CT scans, as long as tumor motion has been taken into consideration at the original simulation and conservative margins and planning strategies have been used for designing the proton plans. However, in selected cases with substantial anatomic and motion changes during 7 weeks of radiation therapy, adaptive re-planning is indicated to keep adequate target coverage and/or to spare normal critical structures.

Acknowledgments

The authors thank all members of the Thoracic Radiation Oncology for their help and support of generic 4D-CT tumor motion study. Supported in part by Grant No. CA74043 from the National Cancer Institute (to X.Z. and R.M.). Dr. Chang is a recipient of the Research Scholar Award from the Radiological Society of North America and a Career Development Award from The University of Texas M. D. Anderson Cancer Center National Institutes of Health Lung Cancer Specialized Programs of Research Excellence (SPORE) P50 CA70907.

REFERENCES

1. Curran W, Scott C, Langer C, et al. Long term benefit is observed in a phase III comparison of sequential vs concurrent chemo-radiation for patients with unresectable NSCLC: RTOG 9410. Proc Am Soc Clin Oncol. 2003:621a.
2. Smith AR. Proton therapy. Phys Med Biol. 2006; 51:R491–R504. [PubMed: 16790919]
3. Schulz-Ertner D, Tsujii H. Particle radiation therapy using proton and heavier ion beams. J Clin Oncol. 2007; 25:953–964. [PubMed: 17350944]
4. Chang JY, Zhang X, Wang X, et al. Significant reduction of normal tissue dose by proton radiotherapy compared with three-dimensional conformal or intensity-modulated radiation therapy in Stage I or Stage III non-small-cell lung cancer. Int J Radiat Oncol Biol Phys. 2006; 65:1087–1096. [PubMed: 16682145]
5. Goitein M, Lomax AJ, Pedroni ES. Treating cancer with protons. Physics Today. 2002; 55:45–50.
6. Jones B, Burnet N. Radiotherapy for the future—protons and ions hold much promise. Br Med J. 2005; 330:979–980. [PubMed: 15860804]
7. Chang, JY.; Mohan, R.; Cox, JD. Image-guided proton radiotherapy.. In: Cox, JD.; Chang, JY.; Komaki, R., editors. Image-guided radiotherapy for non-small cell lung cancer. Informa Healthcare; New York: 2008. p. 127-139.
8. Chang JY, Liu HH, Komaki R. Intensity modulated radiation therapy and proton radiotherapy for non-small cell lung cancer. Curr Oncol Rep. 2005; 7:255–259. [PubMed: 15946583]
9. Liu HH, Balter P, Tutt T, et al. Assessing respiration-induced tumor motion and internal target volume using 4DCT for radiation therapy of lung cancer. Int J Radiat Oncol Biol Phys. 2007; 68:531–540. [PubMed: 17398035]
10. Vedam SS, Keall PJ, Kini VR, et al. Acquiring a four-dimensional computed tomography dataset using an external respiratory signal. Phys Med Biol. 2003; 48:45–62. [PubMed: 12564500]
11. Kang Y, Zhang X, Chang JY, et al. 4D proton treatment planning strategy for mobile lung tumors. Int J Radiat Oncol Biol Phys. 2007; 67:906–914. [PubMed: 17293240]
12. Engelsman M, Rietzel E, Kooy HM. Four-dimensional proton treatment planning. Int J Radiat Oncol Biol Phys. 2006; 64:1589–1595. [PubMed: 16580508]
13. Yan D, Lockman D. Organ/patient geometric variation in external beam radiotherapy and its effects. Med Phys. 2001; 28:593–602. [PubMed: 11339757]
14. Yan D, Wong J, Vicini F, et al. Adaptive modification of treatment planning to minimize the deleterious effects of treatment setup errors. Int J Radiat Oncol Biol Phys. 1997; 38:197–206. [PubMed: 9212024]
15. Britton KR, Starkschall G, Pan T, et al. Assessment of gross tumor volume regression and motion changes during radiotherapy for non-small-cell lung cancer as measured by four-dimensional computed tomography. Int J Radiat Oncol Biol Phys. 2007; 68:1036–1046. [PubMed: 17379442]
16. Ozhasoglu C, Murphy MJ. Issues in respiratory motion compensation during external-beam radiotherapy. Int J Radiat Oncol Biol Phys. 2002; 52:1389–1399. [PubMed: 11955754]
17. Hugo G, Vargas C, Liang J, et al. Changes in the respiratory pattern during radiotherapy for cancer in the lung. Radiother Oncol. 2006; 78:326–331. [PubMed: 16564592]
18. Pan T. Comparison of helical and cine acquisitions for 4D-CT imaging with multislice CT. Med Phys. 2005; 32:627–634. [PubMed: 15789609]
19. Rietzel E, Pan T, Chen GTY. Four-dimensional computed tomography: Image formation and clinical protocol. Med Phys. 2005; 32:874–889. [PubMed: 15895570]
20. Giraud P, Antoine M, Larrouy A, et al. Evaluation of microscopic tumor extension in non-small cell lung cancer for three-dimensional conformal radiotherapy planning. Int J Radiat Oncol Biol Phys. 2000; 48:1015–1024. [PubMed: 11072158]
21. Moyers MF, Miller DW, Bush DA, et al. Methodologies and tools for proton beam design for lung tumors. Int J Radiat Oncol Biol Phys. 2001; 49:1429–1438. [PubMed: 11286851]
22. Enjelsman M, Kooy HM. Target volume dose consideration in proton beam treatment planning for lung tumors. Med Phys. 2005; 32:3549–3557. [PubMed: 16475753]

23. Allen AM, Czerminska M, Jänne PA, et al. Fatal pneumonitis associated with intensity-modulated radiation therapy for mesothelioma. Int J Radiat Oncol Biol Phys. 2006; 65:640–645. [PubMed: 16751058]
24. Bush D, Slater J, Shin B, et al. Hypofractionated proton beam radiotherapy for stage I lung cancer. Chest. 2004; 126:1198–1203. [PubMed: 15486383]
25. Shioyama Y, Tokuuye K, Okumura T, et al. Clinical evaluation of proton radiotherapy for non-small-cell lung cancer. Int J Radiat Oncol Biol Phys. 2003; 56:7–13. [PubMed: 12694818]
26. Nihei K, Ogino T, Ishikura S, Nishimura H. High-dose proton beam therapy for stage I non-small-cell lung cancer. Int J Radiat Oncol Biol Phys. 2006; 65:107–111. [PubMed: 16458447]
27. Chang JY, Dong L, Liu H, et al. Image-guided radiation therapy for non-small cell lung cancer. J Thorac Oncol. 2007; 3:177–186. [PubMed: 18303441]
28. Bosmans G, van Baardwijk A, Dekker A, et al. Intra-patient variability of tumor volume and tumor motion during conventionally fractionated radiotherapy for locally advanced non-small-cell lung cancer: A prospective clinical study. Int J Radiat Oncol Biol Phys. 2006; 66:748–753. [PubMed: 17011450]
29. Kupelian PA, Ramsey C, Meeks SL, et al. Serial megavoltage CT imaging during external beam radiotherapy for non-small-cell lung cancer: Observations on tumor regression during treatment. Int J Radiat Oncol Biol Phys. 2005; 63:1024–1028. [PubMed: 16005575]
30. Bucci MK, Dong L, Liao Z, et al. Comparison of tumor shrinkage in proton and photon radiotherapy of lung cancer. Int J Radiat Oncol Biol Phys. 2007; 69(3 Suppl):S686.
31. Zhang X, Li Y, Mohan R. Use of intensity modulated proton therapy to reduce pneumbra margin. Int J Radiat Oncol Biol Phys. 2007; 69(3 Suppl):S686.

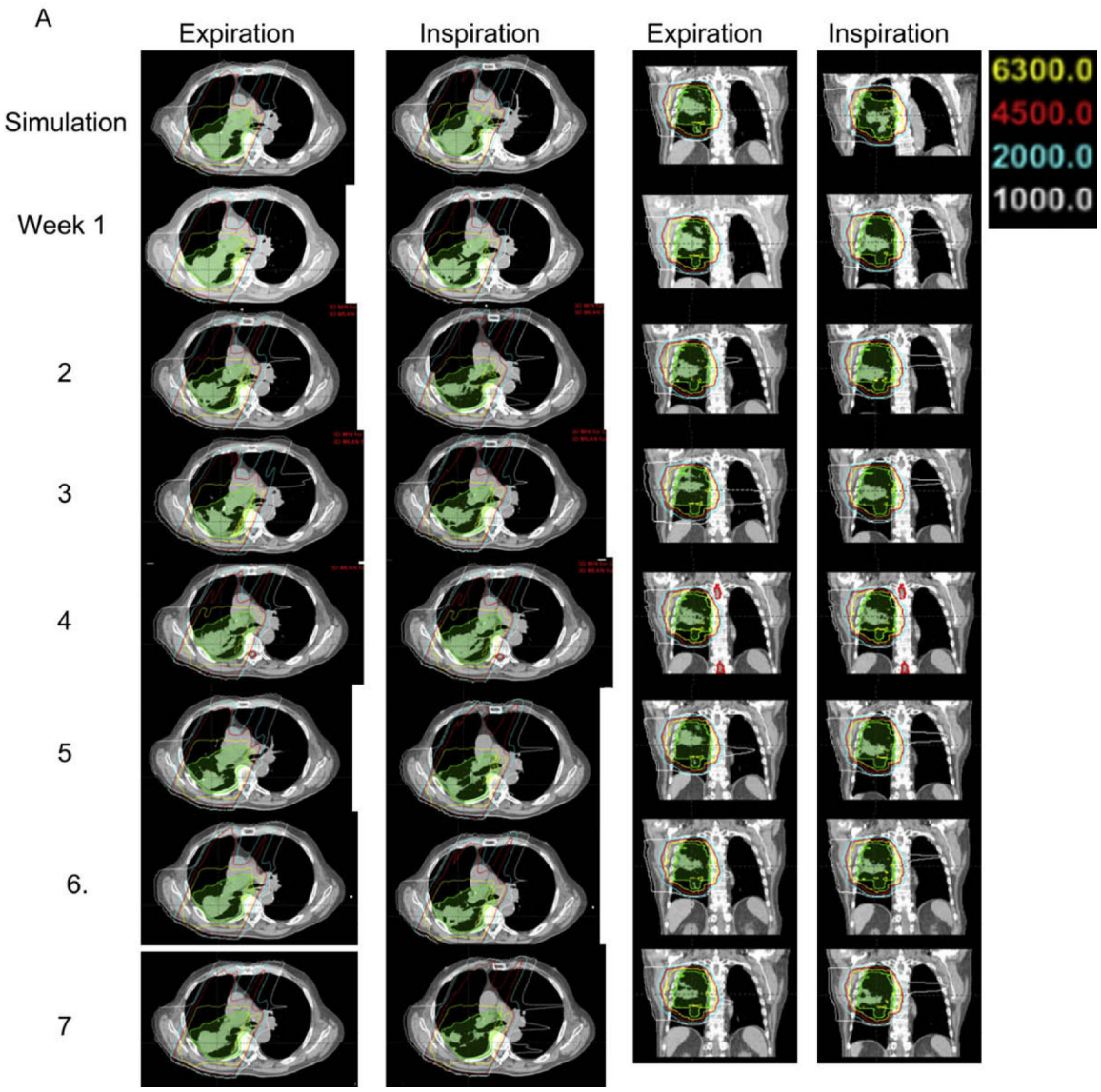

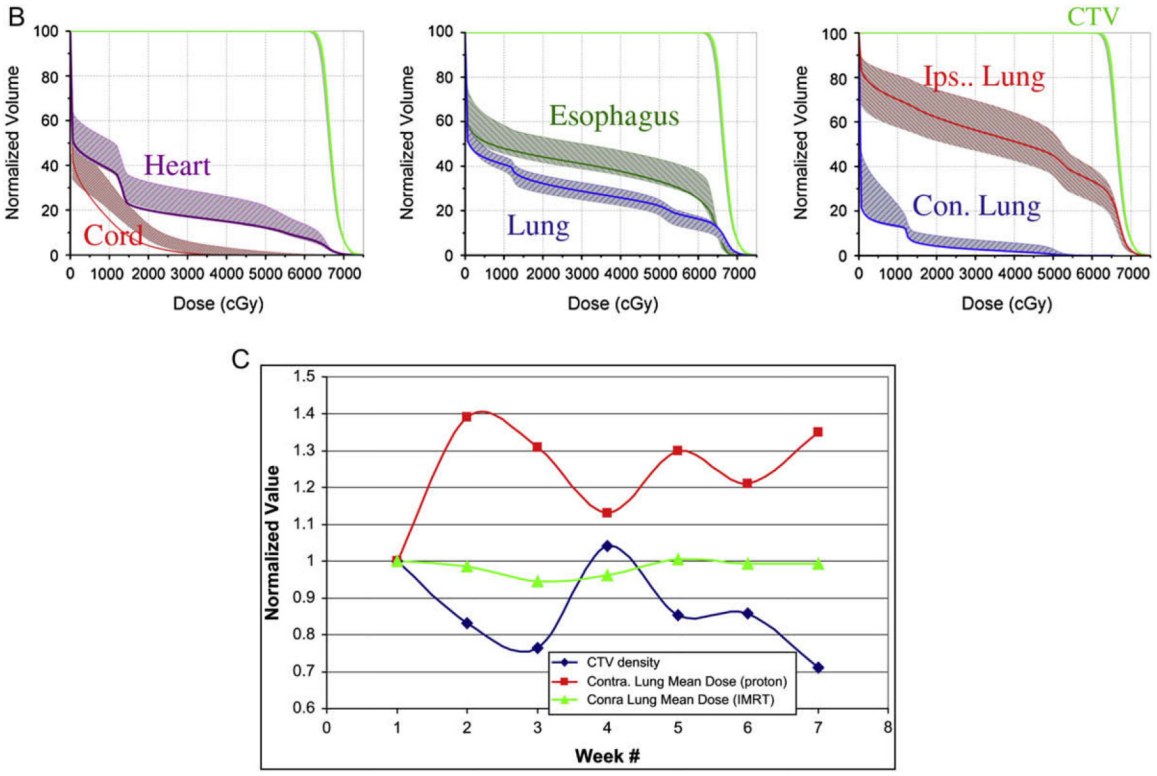

Fig. 1.

Isodose distribution, dose volume and density changes in a typical case during 7 weeks of radiation therapy. (A). The dose distributions in transverse and sagittal planes of the planning computed tomography (CT) scan and seven weekly repeated CT scans in the end-expiration and end-inspiration phases. (B) Dose–volume histograms (DVH) of the clinical target volume (CTV) and normal tissues and their variation (DVH variation band shown as shaded region) over 7 weeks of repeated four-dimensional CT plans. (C) Changes in CTV density correlated inversely with increased contralateral lung mean dose over 7 weeks in proton therapy planning but not in intensity-modulated radiation (photon) therapy planning.

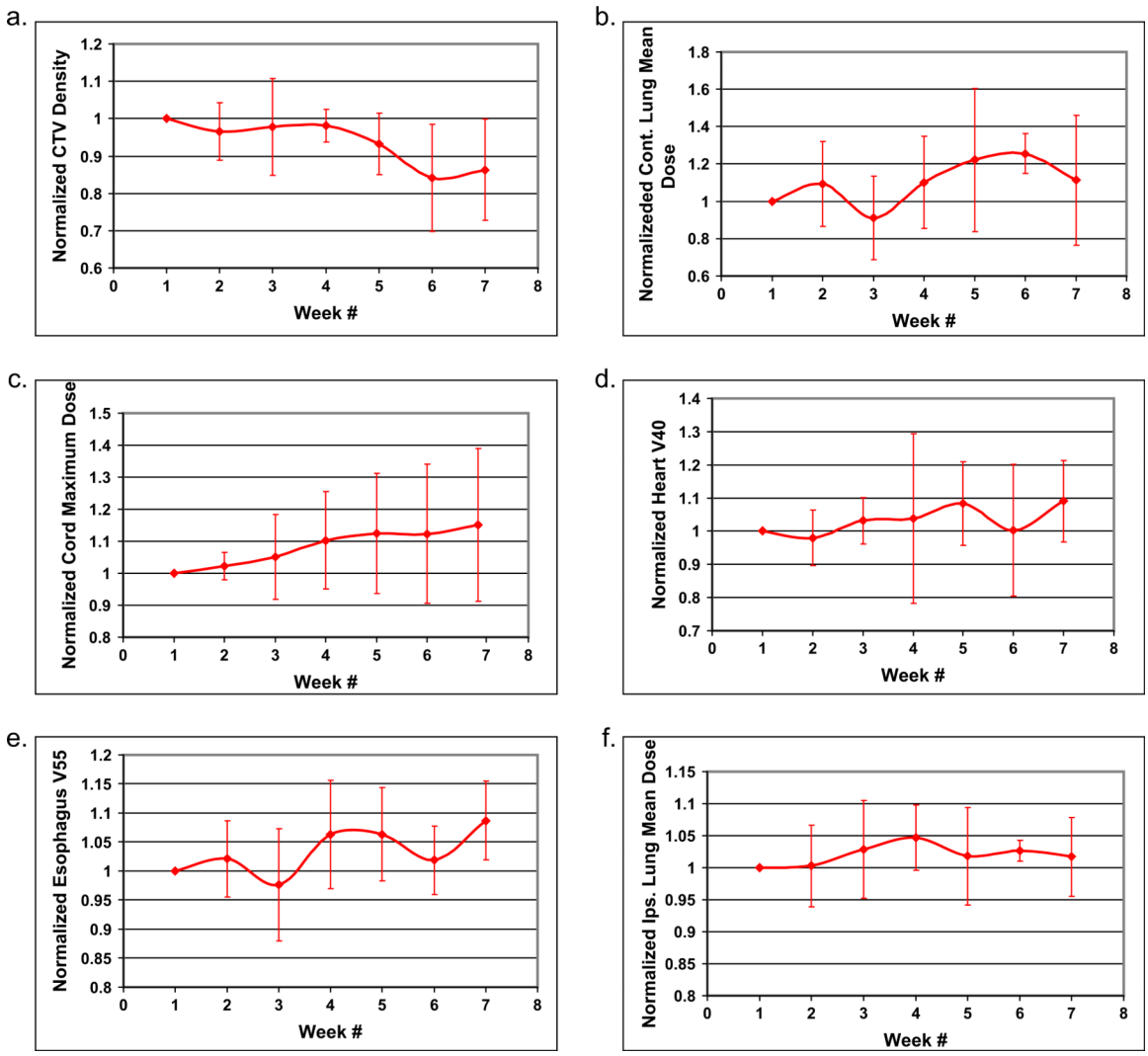

Fig. 2.

Correlation between average scaled clinical target volume (CTV) density change and affected normal tissue endpoints over 7 weeks of radiotherapy for all cases. Average scaled CTV density of (a) contralateral lung mean dose (b), spinal cord maximum dose (c), heart V40 (d), esophagus V55 (e), and ipsilateral lung mean dose (f) for the 8 patients over the 7 weeks of treatment.

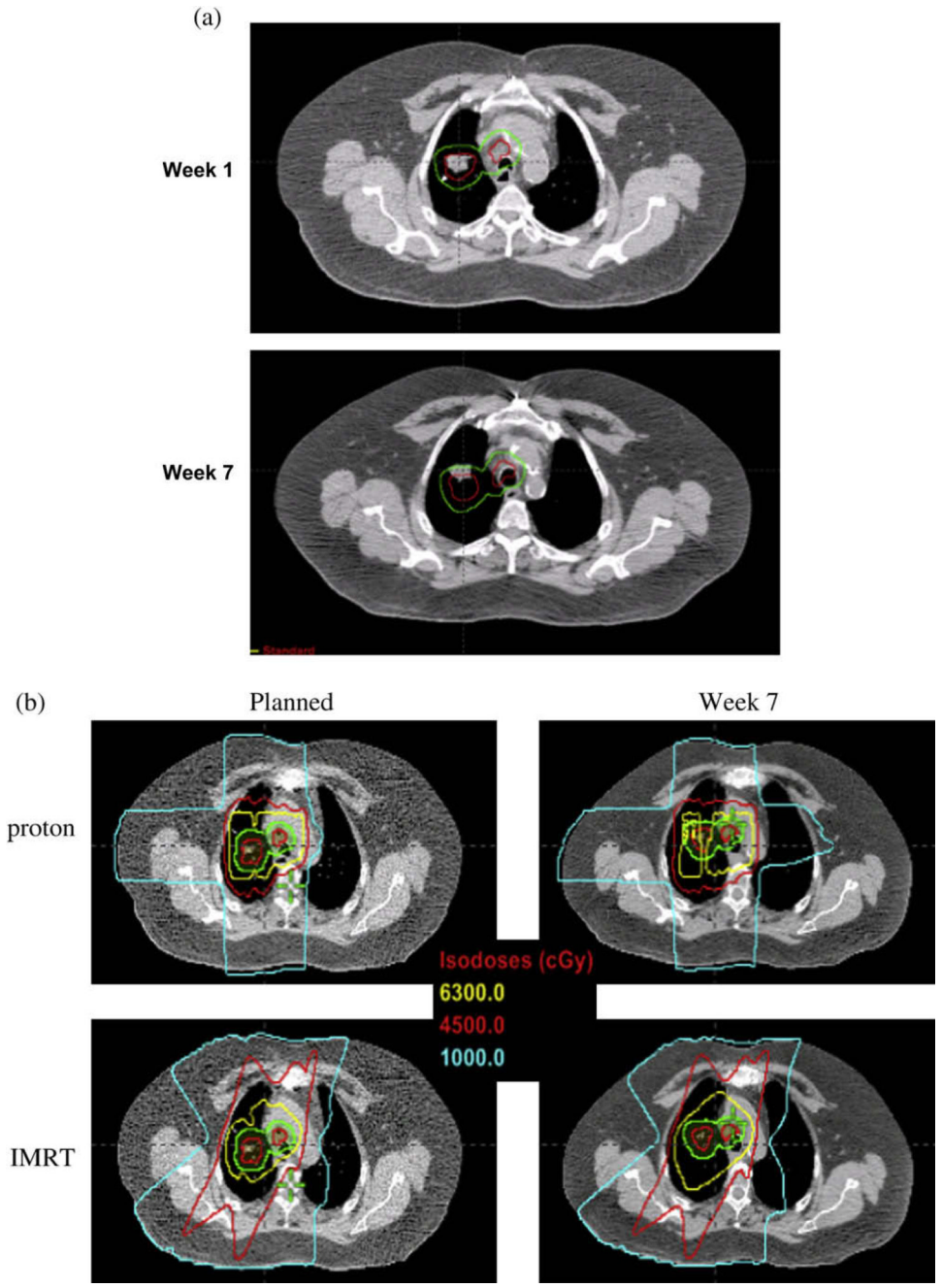

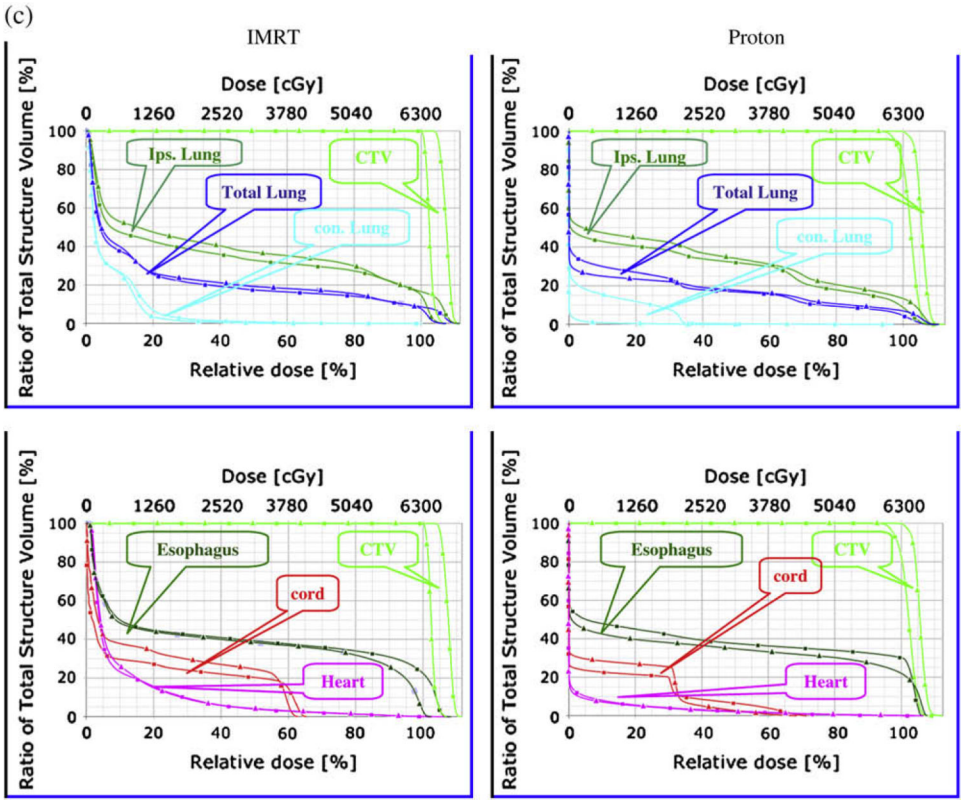

Fig. 3.

Selected case with compromised target coverage and increased normal tissue dose with proton therapy, but not with intensity-modulated radiation therapy (IMRT), caused by significant motion/anatomic changes during 7 weeks of radio-therapy. (a) Target miss caused by motion/anatomic changes. Red line indicates internal gross tumor volume: green line indicates clinical target volume (CTV). Gross tumor volume at 7 weeks moved outside the internal gross tumor volume and CTV contours delineated during four-dimensional computed tomography– based treatment planning. (b) Compromised CTV coverage with prescribed 63 Gy isodose line broken over CTV in proton therapy but not in IMRT. (c) Dose–volume histogram changes between the original plan and 7 weeks after initiation of radiotherapy. Triangle denotes planned; square denotes after 7 weeks treatment.

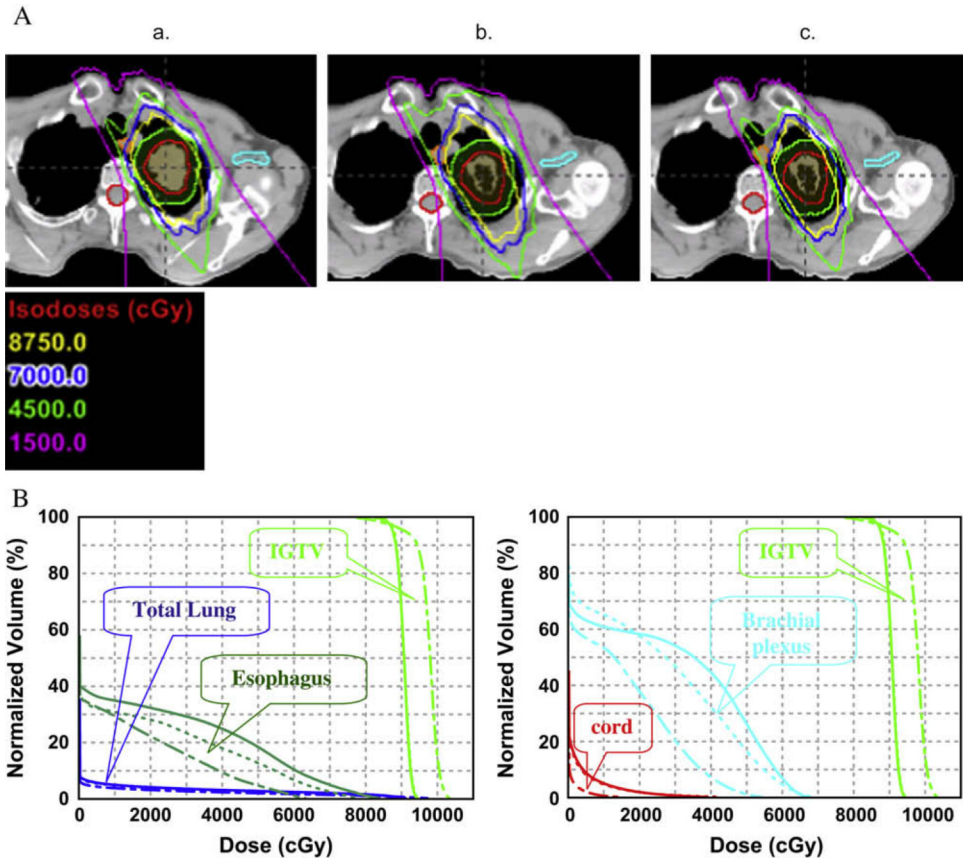

Fig. 4.

Clinical case showing the impact of anatomic changes during proton radiotherapy in clinical target volume (CTV) coverage and critical tissue toxicity in a proton dose-escalated clinical trial. (A) Isodose distribution showed increased normal tissue doses after 5 weeks of proton therapy because of tumor shrinkage and adapted proton plan. (a) Original plan based on simulation four-dimensional computed tomography (4D-CT). (b) Original plan recalculated on basis of 4DCT after 5 weeks of treatment. (c) Re-plan based on CT after 5 weeks of treatment. (B) Dose–volume histograms showing increased normal tissue doses after 5 weeks of proton therapy because of tumor shrinkage and reduced doses resulting from the adaptive proton therapy plan. Dashed line indicates original plan; solid line indicates original plan recalculated based on CT taken after 5 weeks of proton therapy; dot-dashed line indicates re-plan. The dose increased to the brachial plexus (7% over 60 Gy) and esophagus (14% over 55 Gy) at 5 weeks if no re-planning was conducted. However, the adaptive plan reduced the dose to the brachial plexus (<1% over 50 Gy) and the esophagus (<3% over 55 Gy).

Table 1

Dose–volume data for original proton therapy plan and verification using the end of expiration and inspiration phases

	Planed (range)	Expiration (range)	Inspiration (range)	Total (range)
Clinical target volume	99.0 (99.0–99.0)	99.0 (98.6–99.7)	98.9 (98.5–99.3)	98.9 (98.5–99.7)
Total lung				
V5 (%)	36.6 (20.9–56.3)	38.3 (21.3–62.9)	38.3 (20.1–66.9)	38.3 (20.1–66.9)
V10 (%)	34.0 (19.4–52.2)	35.6 (19.7–58.5)	35.6 (18.6–61.6)	35.6 (18.6–61.6)
V20 (%)	30.0 (17.2–16.8)	31.5 (17.5–52.7)	31.1 (16.6–52.9)	31.3 (16.6–52.9)
V30 (%)	25.7 (13.4–10.7)	27.0 (13.4–46.2)	26.5 (13.2–45.3)	26.8 (13.2–46.2)
Mean (Gy)	16.4 (9.3–24.1)	17.1 (9.3–26.8)	17.0 (9.0–26.9)	17.0 (9.0–26.9)
Contralateral lung				
V5 (%)	11.8 (1.1–37.0)	13.2 (1.6–37.0)	15.7 (1.1–37.3)	14.4 (1.1–37.3)
V10 (%)	10.0 (0.8–33.9)	10.9 (0.9–33.8)	13.1 (0.8–34.2)	12.0 (0.8–34.2)
V20 (%)	6.9 (0.3–30.3)	7.7 (0.3–30.1)	8.9 (0.3–30.4)	8.3 (0.3–30.4)
V30 (%)	4.9 (0.0–27.4)	5.5 (0.0–27.2)	6.4 (0.0–27.5)	5.9 (0.0–7.5)
Mean (Gy)	3.8 (0.2–17.5)	4.2 (0.3–17.4)	4.8 (0.2–17.6)	4.5 (0.2–17.6)
Ipsilateral lung				
V5 (%)	59.0 (37.2–89.4)	61.0 (38.9–95.2)	59.0 (34.4–93.6)	60.0 (34.4–95.2)
V10 (%)	55.7 (34.6–85.9)	57.9 (36.1–92.9)	56.1 (32.0–90.5)	57.0 (32.0–92.9)
V20 (%)	50.8 (31.1–80.4)	53.1 (32.5–88.1)	51.4 (28.9–84.8)	52.2 (28.9–88.1)
V30 (%)	44.8 (28.4–71.9)	46.8 (29.6–79.7)	45.2 (26.4–75.8)	46.0 (26.4–79.7)
Mean (Gy)	27.9 (18.6–41.0)	29.0 (19.4–44.7)	28.2 (17.3–43.4)	28.6 (17.3–44.7)
Spinal cord				
Dmax (Gy)	41.7 (34.0–44.7)	41.1 (33.9–44.7)	43.5 (33.9–57.6)	42.3 (33.9–57.6)
D1 (Gy)	32.1 (25.2–35.1)	32.7 (25.2–38.1)	34.7 (25.2–39.1)	33.7 (25.2–39.1)
Heart				
V10 (%)	22.2 (3.1–38.2)	24.2 (5.8–46.2)	22.7 (4.1–42.8)	23.4 (4.1–46.2)
V20 (%)	16.6 (1.3–28.8)	18.3 (3.4–40.1)	17.1 (2.2–35.9)	17.7 (2.2–40.1)
V30 (%)	13.4 (0.3–21.8)	14.7 (1.0–32.3)	13.9 (0.6–28.6)	14.3 (0.6–32.3)
V40 (%)	10.7 (0.1–17.8)	11.8 (0.5–26.6)	11.1 (0.6–72.7)	11.5 (0.3–26.6)
Esophagus				
V30 (%)	42.8 (35.1–52.6)	44.3 (34.7–75.0)	44.3 (34.6–72.7)	44.3 (34.6–75.0)
V40 (%)	39.0 (32.9–46.3)	40.6 (32.5–68.0)	40.5 (31.8–66.0)	40.5 (31.8–68.0)
V55 (%)	32.8 (28.4–38.5)	34.6 (28.0–58.1)	34.0 (26.2–55.0)	34.3 (26.2–58.1)

Table 2

Comparison of dose–volume data between original plan and recalculated, repeated weekly four-dimensional computed tomography plan using alignment with skin marker registration or with bony structure

	Original	Skin registration			Bone registration		
	Planned (range)	Total (range)	Expiration (range)	Inspiration (range)	Total (range)	Expiration (range)	Inspiration (range)
Clinical target volume	99.0 (99.0–99.0)	95.0 (75.5–98.7)	94.5 (75.5–97.9)	95.5 (80.6–98.7)	97.9 (90.9–99.1)	97.5 (90.9–99.1)	98.3 (97.5–99.0)
Total lung							
V5 (%)	36.6 (20.9–56.3)	39.0 (19.2–62.6)	38.3 (19.2–62.6)	39.8 (22.2–59.7)	38.8 (20.0–62.7)	38.2 (20.0–62.7)	39.4 (22.3–60.4)
V10 (%)	34.0 (19.4–52.2)	36.1 (17.8–58.0)	35.1 (17.8–58.0)	37.1 (20.6–56.7)	35.8 (18.6–57.9)	35.0 (18.6–57.9)	36.6 (20.6–57.4)
V20 (%)	30.0 (17.2–46.8)	31.6 (15.9–52.5)	30.3 (15.9–51.2)	32.9 (18.3–52.5)	31.4 (16.7–53.1)	30.3 (16.7–51.0)	32.5 (18.4–53.1)
V30 (%)	25.7 (13.4–40.7)	27.2 (13.4–46.8)	25.8 (13.4–44.2)	28.5 (14.2–46.8)	27.0 (13.7–47.3)	25.8 (13.7–44.1)	28.2 (14.4–47.3)
Mean(Gy)	16.4 (9.3–24.1)	17.3 (8.9–27.3)	16.5 (8.9–26.2)	18.0 (9.9–27.3)	17.1 (9.2–27.4)	16.5 (9.2–26.0)	17.7 (9.9–27.4)
Contralateral lung							
V5 (%)	11.8 (1.1–37.0)	16.0 (0.5–41.7)	18.7 (1.8–40.9)	13.3 (0.5–41.7)	15.8 (0.5–41.5)	18.4 (1.4–40.3)	13.3 (0.5–41.5)
V10 (%)	10.0 (0.8–33.9)	13.2 (0.2–38.2)	15.4 (1.4–37.5)	11.0 (0.2–38.2)	13.0 (0.3–38.0)	15.0 (1.1–36.9)	11.0 (0.3–38.0)
V20 (%)	6.9 (0.3–30.3)	9.0 (0.0–34.0)	10.3 (0.6–33.4)	7.7 (0.0–34.0)	8.9 (0.0–33.8)	10.2 (0.5–32.9)	7.7 (0.0–33.8)
V30 (%)	4.9 (0.0–27.4)	6.1 (0.0–33.4)	10.3 (0.6–33.4)	1.8 (0.0–4.9)	6.0 (0.0–32.9)	10.2 (0.5–32.9)	1.8 (0.0–4.5)
Mean(Gy)	3.8 (0.2–17.5)	4.9 (0.1–19.6)	5.6 (0.3–19.4)	4.3 (0.1–19.6)	4.9 (0.1–19.6)	5.5 (0.3–19.2)	4.3 (0.1–19.6)
Ipsilateral lung							
V5 (%)	59.0 (37.2–89.4)	58.8 (32.9–91.5)	55.4 (32.9–91.5)	62.3 (41.6–79.5)	59.4 (33.4–95.7)	55.5 (33.4–90.5)	63.3 (42.0–95.7)
V10 (%)	55.7 (34.6–85.9)	55.8 (30.6–88.7)	52.5 (30.6–88.7)	59.2 (38.6–78.0)	56.4 (31.1–94.0)	52.5 (31.1–87.7)	60.2 (39.1–94.0)
V20 (%)	50.8 (31.1–80.4)	51.2 (27.7–83.6)	48.1 (27.7–83.6)	54.3 (34.9–74.8)	51.8 (28.1–90.2)	48.2 (28.1–82.8)	55.5 (35.4–90.2)
V30 (%)	44.8 (28.4–71.9)	45.5 (25.5–74.9)	42.8 (25.5–74.9)	48.2 (31.9–68.4)	46.0 (25.8–82.7)	42.7 (25.8–74.3)	49.3 (32.4–82.7)
Mean(Gy)	27.9 (18.6–41.0)	28.1 (16.8–42.8)	26.4 (16.8–42.8)	29.8 (20.7–38.9)	28.3 (16.9–46.6)	26.3 (16.9–42.2)	30.3 (21.0–46.6)
Spine cord							
Dmax(Gy)	41.7 (34.0–44.7)	48.2 (34.8–63.1)	48.2 (34.8–63.1)	48.2 (34.9–62.9)	46.1 (35.1–57.9)	46.7 (36.3–57.9)	45.6 (35.1–56.1)
D1 (cGy)	32.1 (25.2–35.1)	39.4 (31.0–53.8)	39.1 (31.0–53.8)	39.6 (32.6–52.9)	37.4 (31.3–44.0)	37.6 (31.3–43.9)	37.2 (32.0–44.0)
Heart							
V10 (%)	22.2 (3.1–38.2)	25.6 (1.7–48.2)	23.5 (1.7–44.7)	27.7 (10.2–48.2)	24.4 (4.0–46.6)	23.1 (4.0–41.4)	25.8 (6.0–46.6)
V20 (%)	16.6 (1.3–28.8)	19.6 (0.6–41.1)	18.1 (0.6–38.1)	21.2 (7.2–41.1)	18.7 (2.2–40.3)	17.7 (2.2–35.6)	19.6 (3.7–40.3)
V30 (%)	13.4 (0.3–21.8)	15.9 (0.2–33.6)	15.0 (0.2–31.3)	16.9 (2.6–33.6)	15.1 (0.8–32.3)	14.5 (0.8–28.7)	15.6 (2.3–32.3)
V40 (%)	10.7 (0.1–17.8)	12.7 (0.1–28.4)	11.9 (0.1–25.9)	13.6 (1.8–28.4)	12.2 (0.4–26.8)	11.7 (0.4–23.4)	12.6 (1.3–26.8)

	Original	Skin registration			Bone registration		
	Planned (range)	Total (range)	Expiration (range)	Inspiration (range)	Total (range)	Expiration (range)	Inspiration (range)
Esophagus							
V30 (%)	42.8 (35.1–52.6)	43.5 (34.5–57.5)	43.8 (34.5–57.5)	43.2 (36.1–54.3)	43.2 (35.8–58.0)	43.8 (36.1–58.0)	42.7 (35.8–55.6)
V40 (%)	39.0 (32.9–46.3)	36.0 (29.0–43.1)	36.1 (29.0–43.1)	36.0 (29.5–40.4)	35.7 (30.5–44.8)	36.2 (30.5–44.8)	35.2 (30.6–44.0)
V55 (%)	32.8 (28.4–38.5)	33.7 (26.9–41.1)	33.8 (26.9–41.1)	33.6 (27.2–38.1)	33.6 (28.0–42.7)	34.2 (28.0–42.7)	33.0 (28.5–41.5)